Population synthesis of isolated Neutron Stars with magneto-rotational evolution

Miguel Gullón Juanes

in collaboration with: Juan A. Miralles, Daniele Viganò, José A. Pons

The Structure and Signals of Neutron Stars, from Birth to Death
Firenze, 24 March 2014

Universitat d'Alacant
Universidad de Alicante

Outline

Introduction

Motivations

- Observational diversity of Neutron Stars (aka NS Zoo). [Popov (2008)], [Harding (2013)]
- Multiband detections (radio, X,γ-ray, outburst...).
- Open issues (magnetic evolution, EoS, emission, magnetosphere, birth properties...).
- The synthesis of populations could help to get a unifying picture.

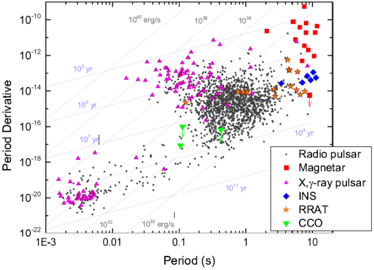

[Harding (2013)]

Population synthesis

Method of direct modeling a population of weakly interacting objects with complex evolution.

Monte Carlo simulations of isolated Neutron Stars: birth, evolution and detection.

Comparison between simulated and observed samples in radio and thermal X-ray bands.

Evolution of rotational properties based on state-of-the-art results of magneto-thermal and magnetospheric models.

Main goals

- Initial parameter constraint (B, P...)
- Model testing
- NS Zoo Unification?

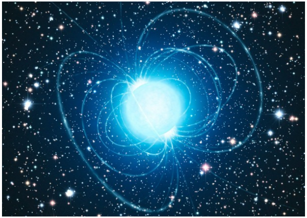

References

Fauchere-Guiguère and Kaspi, 2006.

Popov et al., 2010

Pierbattista et al. 2012

Baseline model

Kinematic properties

Age uniformly chosen in $\rightarrow [0, T_{max}]$ ($T_{max} \sim$ 500 Myr)

Spatial location related to OB associations of massive stars $\rightarrow$ Disk (spiral arms) + height.

Initial velocity ("kick") due to supernova explosion ($\bar{v}_0 \sim 500$ km s^{-1})

Spatial evolution: $\ddot{\mathbf{x}} = -\nabla \phi_{\mathbf{G}}$ [Kuijen & Gilmore (1989)], [Carlberg & Innanen (1987)]

Period, magnetic field and inclination angle

P_0 and $\log B_0$ from normal distributions ($\mu_{B_0}, \sigma_{B_0}, \mu_{P_0}, \sigma_{P_0}$).

Initial inclination angle χ_0 (rotational and magnetic axis) randomly selected.

Evolution dictated by magneto-rotational models.

Radioluminosity and radioflux

$$L_{\rm rad} = L_0\, 10^{L_{corr}} \left(P^{-3}\dot{P}\right)^{\alpha} \sim \dot{E_{rot}}^{\alpha}$$

$$S_{\rm rad} = \frac{L_{\rm rad}}{d^2}$$

Canonical parameters

$M = 1.4\ \mathrm{M}_\odot$

$R = 11.6$ km

Rotational evolution

Neutron Stars increase their periods as intense magnetic fields ($B \sim 10^{13}$) brake their rotation.

In addition to spin-down, some models predict stars to be aligned with time. [Beskin, Istomin & Philippov (2013), Philippov, Tchekhovskoy & Li (2013)]

Rotational evolution:

$$I\frac{d\Omega}{dt} = \mathbf{K} \rightarrow \begin{cases} \dot{\chi} = -\kappa_2 \beta \dfrac{B(t)^2}{P^2} \sin\chi \cos\chi \\ \dot{P} = \beta \dfrac{B(t)^2}{P} (\kappa_0 + \kappa_1 \sin\chi^2) \end{cases} \quad (1)$$

$$\beta = \frac{\pi^2 R^6}{Ic^3} \sim 6 \times 10^{40}\ \mathrm{G}^{-2}$$

$\kappa_i \sim 1.$

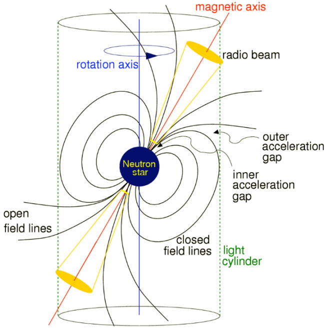

Models

No alignment

Alignment

- Vacuum
- Plasma-filled

Magneto-thermal evolution (J. Pons' talk)

Magneto-thermal evolution

[Viganò et al. (2013)] performed magneto-thermal evolution simulations of NSs.

Most relevant parameters:

- Initial magnetic field B_0
- Impurity parameter in the inner-crust (pasta phase): $Q_{imp} = \langle Z^2 \rangle - \langle Z \rangle^2$

B(t) + Thermal X-ray luminosity L_X

Timescales $\sim$ 1 Myr

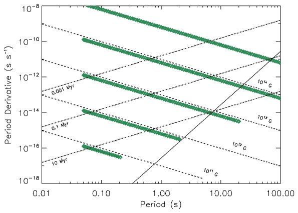

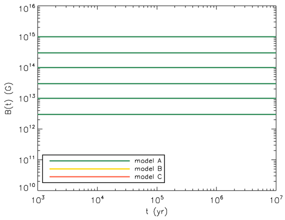

Models

- **Model A. No decay**
- Model B. $Q_{imp} = 25$.
- Model C. $Q_{imp} = 100$.

Magneto-thermal evolution (J. Pons' talk)

Magneto-thermal evolution

[Viganò et al. (2013)] performed magneto-thermal evolution simulations of NSs.

Most relevant parameters:

- Initial magnetic field B_0
- Impurity parameter in the inner-crust (pasta phase): $Q_{imp} = \langle Z^2 \rangle - \langle Z \rangle^2$

B(t) + Thermal X-ray luminosity L_X

Timescales $\sim$ 1 Myr

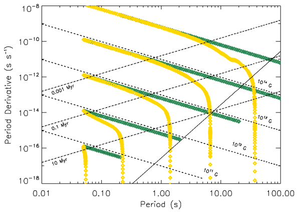

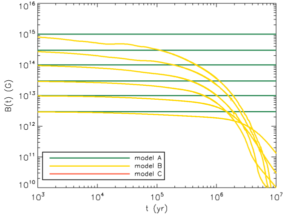

Models

- Model A. No decay
- **Model B.** $\mathbf{Q_{imp} = 25.}$
- Model C. $Q_{imp} = 100.$

Magneto-thermal evolution (J. Pons' talk)

Magneto-thermal evolution

[Viganò et al. (2013)] performed magneto-thermal evolution simulations of NSs.

Most relevant parameters:

- Initial magnetic field B_0
- Impurity parameter in the inner-crust (pasta phase): $Q_{imp} = \langle Z^2 \rangle - \langle Z \rangle^2$

B(t) + Thermal X-ray luminosity L_X

Timescales $\sim$ 1 Myr

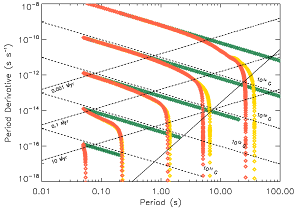

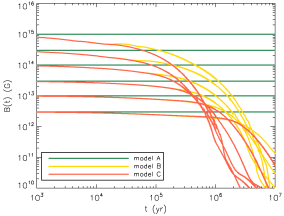

Scenarios

- Model A. No decay
- Model B. $Q_{imp} = 25$.
- **Model C.** $\mathbf{Q_{imp} = 100}$.

Detectability conditions

Radio pulsars

Radio surveys of Parkes (1008) and Swinburne (197) ($\nu \sim 1400$ MHz).

Beaming factor: $f = 9[\log(P/10s)]^2 + 3$ [Tauris & Manchester (1998)]

Minimum flux: S_{min} [Dewey et al. (1984)]

Limited area of sky.

Detectability conditions

Radio pulsars

Radio surveys of Parkes (1008) and Swinburne (197) ($\nu \sim 1400$ MHz).

Beaming factor: $f = 9[\log(P/10\mathrm{s})]^2 + 3$ [Tauris & Manchester (1998)]

Minimum flux: S_{min} [Dewey et al. (1984)]

Limited area of sky.

X-ray thermal NSs

NS cooling catalog [a] (~ 40) (D. Viganò's talk)

Blackbody isotropic emission: $F_X = \dfrac{L_X}{4\pi d^2}$

Interstellar absorption model [Balucinska-Church et al.,1992]

Minimum flux $F_{Xmin} = 10^{-14} \mathrm{ergs}^{-1} \mathrm{cm}^{-2}$

All-sky coverage.

[a] http://www.neutronstarcooling.info/

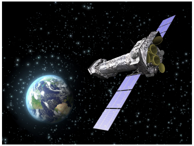

Search for optimal parameters

Main parameters

$[\mu_{P_0}, \sigma_{P_0}, \mu_{B_0}, \sigma_{B_0}]$, α, Q_{imp}, alignment (ON/OFF).

Each synthetic sample have associated the statistic D from a 2 dimensional-KS test. This value accounts for the similarity between the observed and simulated samples.

Simulated annealing method

In order to look for optimal fits we have implemented an algorithm that minimizes the D value.

It is based on random walks that look for the minimum energy state (analogy of cooling down of liquids that become crystals).

Degeneracy of parameter space

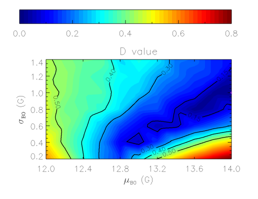

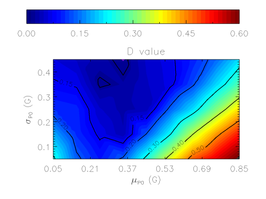

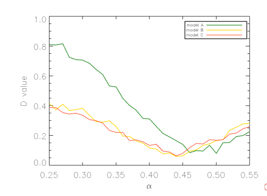

Radio pulsars

Observed

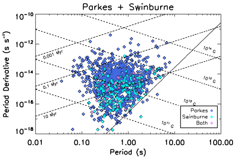

Magnetothermal evolution models

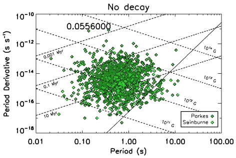

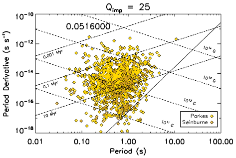

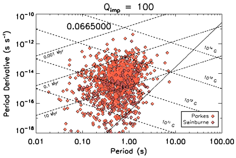

Radio pulsars

Observed

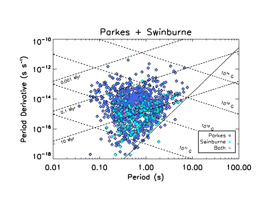

Alignment models

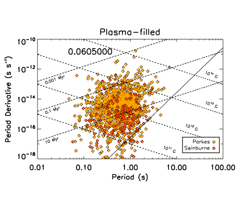

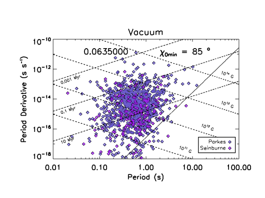

Magnetothermal evolution models

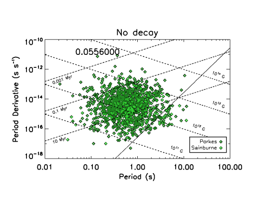

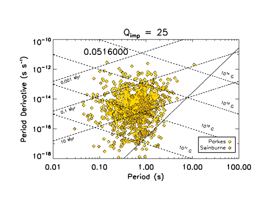

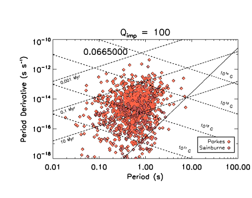

X-ray thermal NSs

Magnetothermal evolution models

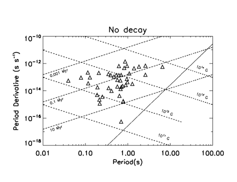

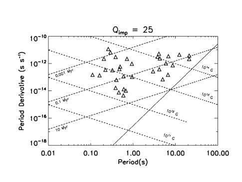

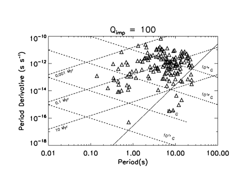

Observed

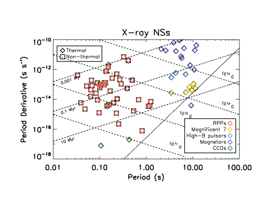

Constant magnetic field has a lack of high-B sources detected while the extreme decay model ($Q_{imp} = 100$) produces too many.

The intermediate decay model ($Q_{imp} = 25$) leads to a gap that is also observed in the catalog.

Conclusions and Future work

Discussion

We have performed population synthesis studies on isolated Neutron Stars. We look for best match solutions in the radio and X-ray bands. Different magneto-rotational models have been tested.

In the radio band the parameter space seems to be **degenerated** as several set of parameters lead to proper soutions.
Both constant magnetic field and decay models reproduce quite well the bulk of the radio pulsar population. However, there are many sources beyond the death-line and no detections with lower $\dot{P}$ for the constant magnetic field model.
The inclusion of alignment do not introduces variations in pulsars with plasma-filled magnetospheres. For vacuum magnetospheres, the stars must be born as ortogonal rotators.

The inclusion of X-ray band could partially remove the degeneracy encountered.

More constraints (birth rate, other bands...) will be studied in the near future.

Conclusions and Future work

Discussion

We have performed population synthesis studies on isolated Neutron Stars. We look for best match solutions in the radio and X-ray bands. Different magneto-rotational models have been tested.

In the radio band the parameter space seems to be **degenerated** as several set of parameters lead to proper soutions.
Both constant magnetic field and decay models reproduce quite well the bulk of the radio pulsar population. However, there are many sources beyond the death-line and no detections with lower $\dot{P}$ for the constant magnetic field model.
The inclusion of alignment do not introduces variations in pulsars with plasma-filled magnetospheres. For vacuum magnetospheres, the stars must be born as ortogonal rotators.

The inclusion of X-ray band could partially remove the degeneracy encountered.

More constraints (birth rate, other bands...) will be studied in the near future.

Future work

Gamma-ray pulsars & X-ray non-thermal NSs.

Outburst mechanisms.

Binaries?


THANK YOU!

Search for optimal parameters

2D KS test

[Fasano & Franceschini (1987)]

Comparison between observed and simulated $(P, \dot{P})$.

Generalized D value $\rightarrow$ Integrated probability in four natural quadrants around each point.

Statistical error $\Delta_{stat} \sim 0.01$.

Probability of similarity: $p(D > D_{obs}) = Q_{KS}\left(\frac{\sqrt{N}D}{1+\sqrt{1-r^2}(0.25-0.75/\sqrt{N})}\right)$.

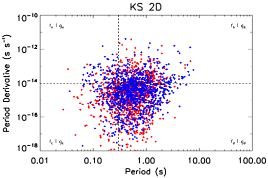

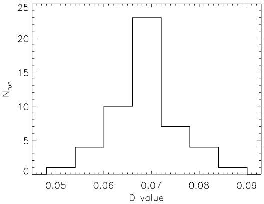

Radioluminosity + Beaming

Radioluminosity

Uncertainties related to pulsar emision mechanism.

Numerous fits for $L_{\rm rad} = \begin{cases} a\, P^p\, \dot{P}^q \\ L_0^{\gamma} \end{cases}$

No observed correlation in real data. Weak correlation or strong selection effects?

Random luminosity produces pile-up towards death-line. [Faucher-Guigere & Kaspi (2006)]

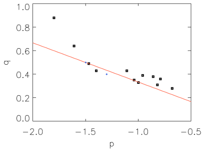

[Bagchi (2013)]

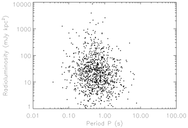

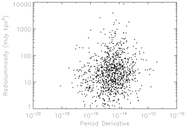

Beaming factor: $f = 9[\log(P/10{\rm s})]^2 + 3$ [Tauris & Manchester (1998)]

$$L_{\rm rad} = L_0\, 10^{L_{corr}}\, (P^{-3}\dot{P})^{\alpha} \sim \dot{E_{rot}}^{\alpha}$$

$$S_{\rm rad} = \frac{L_{\rm rad}}{d^2}$$